

Sublimative desorption of xenon from Ru(100)

Gabriel Kerner, Ori Stein, Yigal Lilach, and Micha Asscher*

Department of Physical Chemistry, The Farkas Center for Light Induced Processes, The Hebrew University of Jerusalem, Jerusalem, 91904 Israel

(Received 19 December 2004; published 26 May 2005)

Sublimative desorption is a process in which desorption of multilayers of an adsorbate precedes melting and surface diffusion. Here we report on the desorption kinetics of Xe atoms from multilayer coverage studied using temperature programmed desorption and optical diffraction methods. It is found that decay of the diffraction peak intensities from multilayer coverage grating during surface heating cannot be explained as one-dimensional diffusion process. Instead, the diffraction signal follows Xe desorption, as deduced from simultaneous linear diffraction and desorption measurements. This observation suggests that no macroscopic two-dimensional melting and diffusion occur in the case of multilayers of Xe before the onset for desorption. It is concluded that Xe atoms undergo sublimative desorption from the topmost layers. Similar results were obtained in the case of water multilayers on Ru(100). These results suggest that on solid surfaces the desorption of multilayers is thermodynamically favorable over surface melting or diffusion.

DOI: 10.1103/PhysRevB.71.205414

PACS number(s): 68.43.-h, 81.15.-z, 81.16.-c

I. INTRODUCTION

Desorption kinetics of submonolayer Xe coverages from well-defined metallic surfaces has been extensively studied by several groups, both experimentally and from the theoretical point of view.¹⁻¹¹ It can serve as model system for gas-surface interaction, and for atomic adsorption. Menzel and co-workers have studied in great detail several Xe/metal systems and concluded from the analysis of temperature programmed desorption (TPD) that Xe desorbs from metallic substrates via zero-order kinetics up to multilayer coverages.^{1,3,4} Observation of zero-order kinetics at submonolayer coverage has often been rationalized by an adsorbate system consisting of two-dimensional (2D) islands. These islands coexist in a quasi-equilibrium with single atoms within a “dilute” 2D gas.^{6-10,12-15} Both the 2D condensed phase and the 2D gas are in direct contact with the substrate. This model is generally applicable for submonolayer coverages. Asada *et al.* presented a bilayer model for zero-order desorption,¹³ where the two adsorbed phases do not coexist anymore in a single layer, rather in a double layer consisting of a first dense layer, and a second, more dilute one.

The diffusion of submonolayer Xe on metallic surfaces has been studied as well in recent years. Understanding the diffusion of rare gas atoms on metals continues to serve as model for crystal growth and surface diffusion processes in general. Employing the hole refilling method by laser induced thermal desorption (LITD), George and co-workers have investigated the submonolayer xenon diffusion on a stepped Pt(11,11,9) surface.¹⁶ Both the diffusion and desorption rates were found to be independent of Xe coverage. A relatively high barrier for diffusion of 2.8 kcal/mol was reported, considering that the activation energy and heat of vaporization for multilayer desorption are 3.6 ± 0.2 kcal/mol.^{1,3,4} These authors concluded that both diffusion and desorption originate from 2D islands. In a more recent study, Thomas *et al.* used linear diffraction from a Xe coverage grating to follow the submonolayer diffusion on a

Nb(110) surface, and found a barrier for diffusion of only 1.25 kcal/mol.¹⁷ However, to our knowledge, no study to date has addressed the 2D melting and diffusion of multilayer xenon on surfaces.

In addition to its basic importance, the desorption and diffusion kinetics of multilayer Xe on surfaces plays an important role in buffer layer assisted growth¹⁸⁻²² and laser patterning²³⁻²⁶ of metals on surfaces. Used as physisorbed buffer layer between the substrate and metal to be deposited, it induces the formation of abrupt interfaces, resulting in the growth of metallic nanoclusters on any substrate, whose size can be controlled by variation of thickness of the Xe buffer layer. It is also the basis for the formation of well-defined submicron range variable width metallic wires, employing LITD of the Xe buffer layer and the metal layer on top. Understanding the diffusion and desorption kinetics of multilayer Xe can therefore provide critical information on the coalescence and deposition mechanism of the metal film on a surface, and the parameters that control it.

Optical linear diffraction from a coverage density modulation (grating) over a solid substrate prepared via LITD is a macroscopic method well suited for the investigation of rare gas diffusion.^{27-30,17} This method, combined with simultaneous mass spectrometry, is the focus of this work, where we have investigated the desorption and diffusion kinetics of multilayer Xe and that of water on Ru(100) single crystal surface.

II. EXPERIMENT

The experimental setup was described in detail elsewhere.^{23,24,31} Briefly, an ultrahigh vacuum chamber at a base pressure of 3×10^{-10} mbar was used, equipped with a 600 eV Ne⁺ sputter gun for sample cleaning, a quadrupole mass spectrometer (QMS) for temperature programmed desorption (TPD), LEED, and a Kelvin probe for work function change measurements. The mass spectrometer was enclosed in a glass shroud that could be brought to within 1 mm

(± 0.05 mm) from the sample surface. The Ru(100) sample [6.5 mm diameter, 1 mm thickness oriented within 0.1° from its (100) crystallographic plane] was mounted on a cryogenic cold head (APD Inc.), with minimum sample temperature of 20 K. Temperature measurements were performed using a calibrated W26%Re vs W5%Re thermocouple junction, spot welded to the sample edge.³² It was calibrated against ΔP -TPD of multilayer CO at a heating rate of 1 K/s. The TPD was found identical to that previously published in the literature.⁴ Temperature control is achieved by resistively heating the metallic sample, with thermal stability of about ± 0.3 K, and absolute accuracy of about ± 1 K over the temperature range 20–1000 K. After sputter cleaning and flash heating to 1620 K, the sample was cooled back to 20 K and exposed to Xe gas (99.999% pure), by back filling the chamber to (5×10^{-9} – 5×10^{-8}) mbar Xe. An attempt to use a capillary dozer resulted in experimental artifacts apparently due to inhomogeneous coverage on the surface.

Diffusion measurements were performed by monitoring the decay of the first-order optical linear diffraction signal generated by Xe periodic coverage density modulation (grating), as a function of surface temperature. A *p*-polarized pulsed Nd-YAG laser (10 ns pulse duration) at its fundamental wavelength of 1064 nm was used for coverage grating formation via LITD.^{23–31} It was formed by overlapping a split laser pulse on the sample surface at an angle of $\theta = \pm 6.0^\circ$ with respect to the surface normal, resulting in coverage grating period of 5 μm . Absorbed laser power density was typically 2 MW/cm², equally divided between the two overlapping beams. During the grating formation process, the laser pulse that strikes the sample causes a sudden pressure burst in the vacuum chamber, which is proportional to the initial Xe multilayer coverage. This can be used as an indirect calibration of the Xe layer thickness. The probe laser for optical linear diffraction²⁷ was a cw 5 mW nonfocused, *p*-polarized HeNe Laser, at incident angle of 50° . The cw probe beam did not affect in any way the substrate temperature. Its effect on the diffusion measurements can therefore be neglected.

Simultaneous measurements of the optical linear diffraction intensity and TPD were performed. The decay of the first-order linear diffraction signal caused by evaporation of the periodic coverage modulation was recorded while the quadrupole mass spectrometer monitored the desorption of Xe atoms from the surface, both during surface temperature ramp.

III. RESULTS AND DISCUSSION

A. Desorption experiments

TPD spectra of Xe from the Ru(100) surface were recorded for different initial Xe coverages, at a linear heating rate of 1 K/s (Figs. 1 and 2). The desorption spectra are typical and look similar to those reported previously in the literature over the hexagonal Ru(001) surface.⁴ The first monolayer of Xe desorbs from the ruthenium surface around 93 K. Unlike the desorption kinetics of Xe from the Ru(001) surface, it does not obey zero-order kinetics on the Ru(100) surface as deduced from the relevant submonolayer TPD line

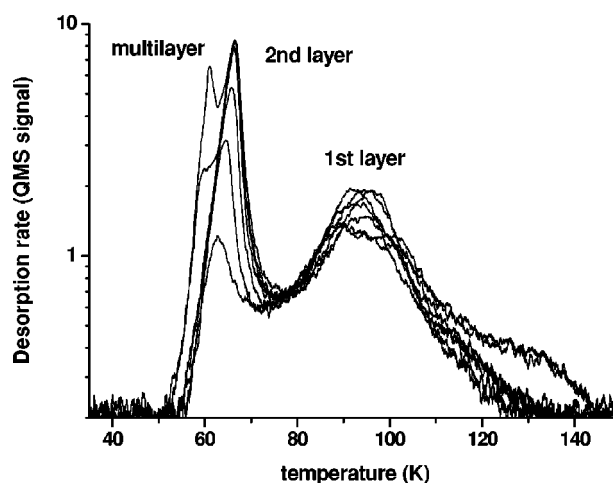


FIG. 1. TPD of 1.2–2.5 ML Xe from Ru(100), performed at a heating rate of 1 K/s.

shapes. In addition, the spectrum quality depends on background gases. For example, trace desorption from the surface is observable at a temperature higher than the peak desorption temperature, with a small desorption hump at 135 K. This peak is sensitive to the crystal quality, i.e., before or after sputter cleaning and flash heating to 1620 K. This high temperature peak vanishes in the presence of coadsorbed CO and H₂ impurities that may block such defect sites. The activation energy for desorption of the first layer is (6.3 ± 0.1) kcal/mol, with a preexponential factor of 1×10^{12} s⁻¹. These values are obtained from full TPD line shape analysis.⁴ The second layer is well separated from the multilayer peak, desorbing between 57 and 67 K, and is characterized by an activation energy for desorption of 3.9 kcal/mol, with a preexponential factor of 1×10^{13} s⁻¹. Recent LEED experiments suggested a phase transition between the second adsorbed Xe layer and those above it.¹¹ Similar behavior was experimentally observed also in the TPD of Xe from Pt(997).¹

Onset for the desorption of third and thicker Xe layers (multilayer) is observed already at 55 K. It fits well zero-

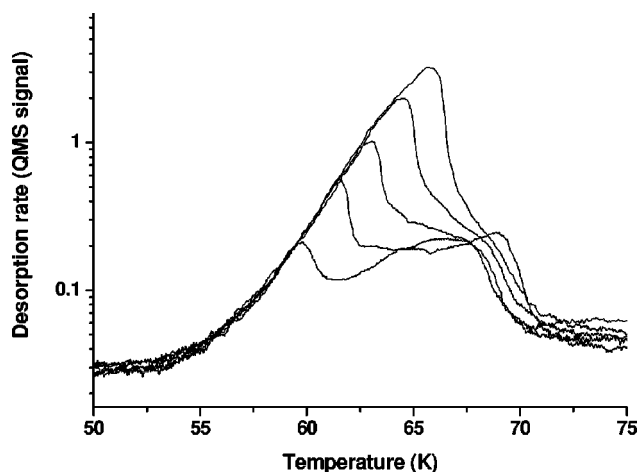


FIG. 2. TPD of multilayer Xe from Ru(100), in the range 3.5–12 ML xenon, at a heating rate of 1 K/s.

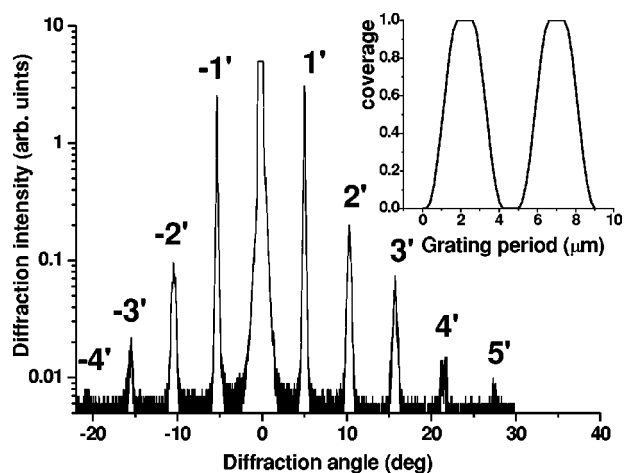


FIG. 3. Optical linear diffraction spectrum obtained from 60 ML Xe coverage grating. Incident angle between the LITD laser beams was 6° , and incident angle of the He-Ne (5 mW) laser for detection was 50° . The inset shows the (normalized) coverage grating profile obtained from Fourier analysis of the diffracted peak intensities.

order desorption kinetics, as shown in Fig. 2, with an activation energy of (3.5 ± 0.1) kcal/mol, assuming a preexponential factor of 1×10^{13} ML/s, in agreement with previous studies on other metallic surfaces and the heat of sublimation from solid Xe.¹⁻⁴ As coverage increases, the desorption peak overlaps the second layer peak, resulting in a broad TPD spectrum.

B. Diffusion measurements

Understanding the mechanism of multilayer Xe diffusion may contribute to our ability to manipulate and control the growth of metallic layers deposited on top.¹³⁻¹⁸ An attempt to measure the diffusion of multilayer Xe over micrometer range requires one to record optical linear diffraction spectra from a multilayer coverage grating. The formation of such adsorbate grating was explained in Sec. II, with further details in Refs. 23 and 24. A diffraction spectrum from such a coverage density modulation at 20 K is shown in Fig. 3. Based on standard simulations of the LITD process^{33,34} using desorption kinetics parameters of the multilayer Xe from Ru(100), we could generate coverage grating profiles that produce qualitatively similar diffraction pattern, via Fourier analysis, as in the experiment. An example of a calculated profile of this kind is demonstrated in the inset of Fig. 3 (the coverage scale is normalized to the full multilayer of 60 ML Xe).

Beginning with a Xe coverage grating on the surface, diffusion is expected to commence by gradually filling the periodic troughs, thus smearing out the overall grating profile in time, as schematically described in Fig. 4(a). One can follow the diffusion process by recording the decay of high order diffraction peaks. The one-dimensional Ficks' second diffusion equation dictates that in the case of one-dimensional diffusion (perpendicular to the troughs), the first-order diffraction signal should decay exponentially, as long as the lateral interactions among neighbors can be ignored:^{27,33-36}

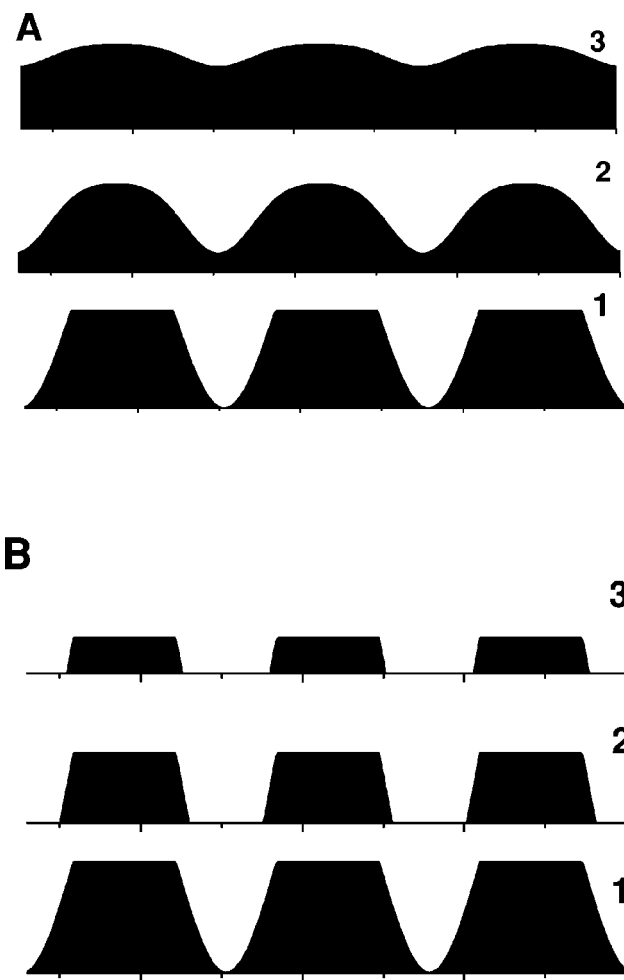


FIG. 4. Schematic diffusion mechanism vs desorption of multilayers Xe on surfaces: (a) From an initial coverage grating (1) one expects a gradual filling of the grating troughs (2) eventual smearing out of the periodic modulation (3). (b) From an initial coverage grating (1), the Xe desorbs only from the outer layer, therefore the grating profile shrinks and the troughs become effectively wider (2), finally the Xe layer thickness fully shrinks (3).

$$\frac{\partial \theta(x)}{\partial t} = \frac{\partial}{\partial x} \left\{ D[\theta(0)] \frac{\partial \theta(x)}{\partial x} \right\}. \quad (1)$$

In the case of multilayer Xe as in this case, $\theta(0)$ represent the full multilayer coverage. The diffusion coefficient in such cases is expected to be independent of the layer thickness. The n th Fourier component of the adsorbate density grating squared is proportional to the experimentally determined optical linear diffraction signal:²⁷

$$S_n(t) = S_n(t=0) \exp(-2\pi^2 n^2 D t / w^2), \quad (2)$$

where $S_n(t)$ is the signal intensity at time t , $S_n(t=0)$ the initial signal intensity, n the diffraction order, w the grating period determined by Bragg equation ($w = \lambda / 2 \sin \theta$), and D is the chemical diffusion coefficient.

Isothermal decay curves of the first-order optical linear diffraction signal at different temperatures in the range 55–60 K are shown in Fig. 5, all at identical initial Xe cov-

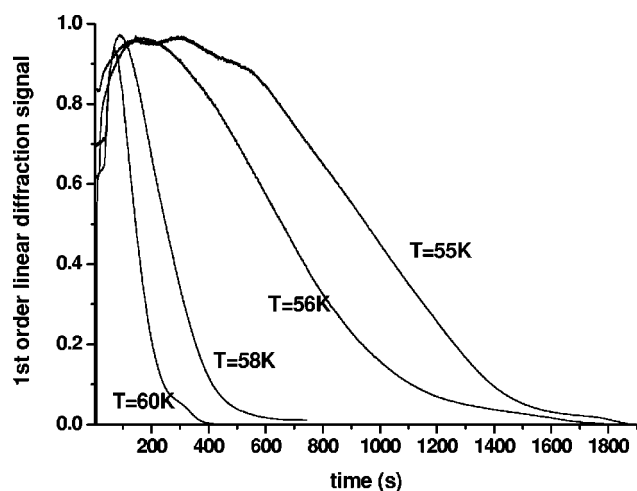


FIG. 5. Isothermal decays of the first-order optical linear diffraction peak from a Xe coverage grating at the indicated desorption temperatures. The spectra cannot be fitted to a single or double exponent, as expected for surface diffusion, see the text.

erage of 60 ML. The diffraction signal initially increases before decay takes over. It seems to correlate with the width of the grating troughs that is dictated by the laser power. At laser power above 4 MW/cm^2 this initial increase vanishes. The decay has an initial temperature-dependent linear section that changes into an exponential form at longer times (see Fig. 5).

Generally, diffusion of adsorbates on surfaces at submonolayer coverages initiates at temperatures well below desorption temperatures, as the activation energy for diffusion is usually lower than that for desorption.³⁷ For example the onset for micrometer scale diffusion of submonolayer coverage of CO on Pt(111)³⁸ is below 150 K while desorption does not take place before 400 K. Similarly, K on $\text{Cr}_2\text{O}_3(0001)$ diffuses at 200 K while the onset for desorption

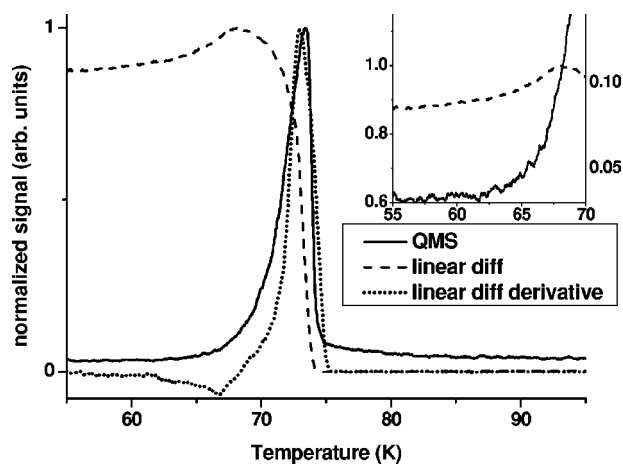


FIG. 6. Xe TPD at a heating rate of 1 K/s, combined with optical linear diffraction signal and its derivative. Initial Xe deposition was of 60 ML, followed by Xe coverage grating formation via LITD. The derivative of the diffraction signal suggests that the linear diffraction follows desorption rather than diffusion. Inset: Desorption onset vs linear diffraction intensity change.

is only above 300 K.³¹ Similar behavior is also observed for the LITD diffusional refilling of Xe on the stepped Pt(11,11,9), where submonolayer diffusion over micrometer range starts already near 55 K while desorption onset is only at 85 K.¹⁶ In contrast, the Xe multilayer system stays immobile up to very close to the desorption temperature. As a result there is practically no change in the first-order signal intensity at temperatures below the onset for Xe desorption. The temperature at which the decay of the first-order diffraction peak initiates, coincides with the onset for multilayer Xe desorption. Moreover, from the spectra shown in Fig. 5 it is evident that the signal does not follow any single or double exponential decay, as expected from the second Fick diffusion equation. This suggests that the diffraction signal follows desorption that takes place directly from the Xe troughs, rather than “melting” and diffusion of the multilayer Xe on the Ru surface. This is schematically shown in Fig. 4. The small hump observed at the initial stages of the decay shown in Fig. 5 (for cases where the grating generation laser power was kept below 4 MW/cm^2) may then be explained by Xe desorption from the coverage grating [Fig. 4(b)]. The desorption process that takes place at the outermost layer of the patterned Xe, leads to an effective widening of the ablated grating troughs. According to LITD coupled to Fourier analysis this leads to an enhancement of the first-order optical diffraction signal, as detected, before decay takes over and dominates.

C. Diffusion versus desorption

In order to better understand the origin of the decay curves presented in Fig. 5, simultaneous detection of the two competing processes of multilayer melting/diffusion and desorption was set-up. Following Xe coverage grating formation, the sample was rotated in front of the quadrupole mass spectrometer (QMS). The first-order linear diffraction signal was recorded at an angle of incidence of 50° , while the sample temperature was ramped. This way TPD and optical diffraction were simultaneously measured to ensure accurate temperature recording for both processes.

Two spectra of this kind are demonstrated in Fig. 6, employing laser power of 2.5 MW/cm^2 over 60 ML Xe. Both signals were normalized to their respective maximum signal intensity for clarity purposes. The derivative of the diffraction signal (normalized) as a function of temperature was also plotted together with the original signals. As discussed earlier, there is no change in the first-order diffraction signal up to the Xe desorption onset near 60 K, as magnified in the inset of Fig. 6. The diffraction signal changes (initially rising then it decays) only as the QMS intensity rises, i.e., as Xe desorbs and its coverage on the surface gradually vanishes. The linear diffraction signal emerges as an early, noninvasive and convenient probe for the desorption of multilayer xenon.

A clear indication of the sublimative desorption behavior of Xe is revealed by plotting the first-order diffraction derivative together with the Xe TPD. The derivative peak coincides with the desorption peak at 73 K. The disappearance of the grating pattern cannot, therefore, arise from smearing out its coverage modulation as a result of 2D melting or

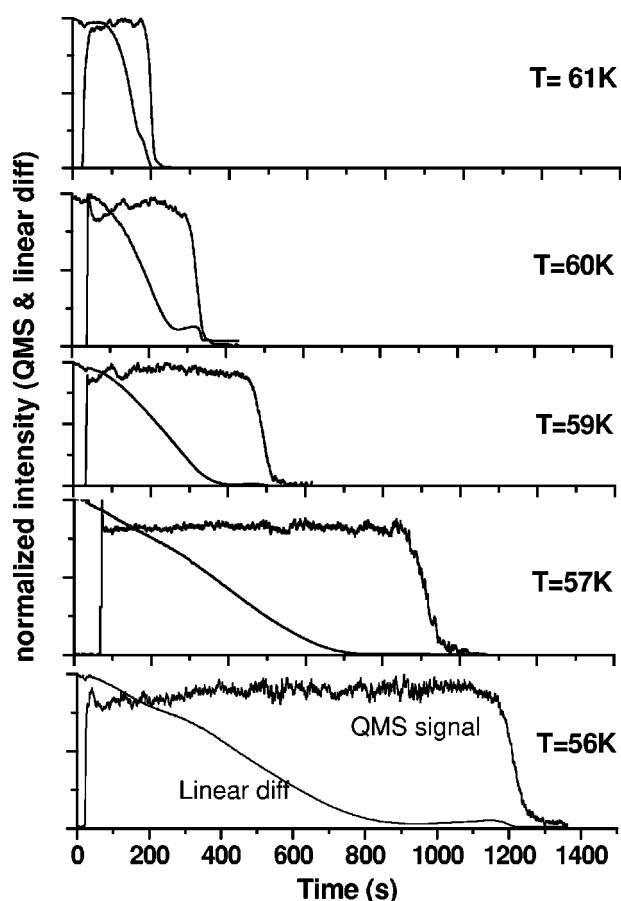


FIG. 7. Isothermal desorption vs the first-order linear diffraction from a multilayer Xe coverage grating, at the indicated temperatures. Initial Xe coverage was 100 ML, heating rate from 20 K to the indicated temperature used for isothermal desorption was 3 K/s.

lateral diffusion, but rather it is due to evaporation of the Xe layers, as expected in the case of sublimative desorption event.

Isothermal desorption experiments were performed in order to confirm the sublimative desorption nature of multilayer xenon. Combined with linear diffraction measurements from the xenon coverage grating, isothermal desorption spectra of 100 ML xenon at different temperatures were recorded. The results are displayed in Fig. 7. Constant desorption rate (time invariant QMS signal) has been observed, consistent with zero-order desorption kinetics. The overall integral of the signal intensity is equal for all graphs, corresponding to the desorption of 100 ML Xe. However the intensity of the QMS signal, and the overall desorption time (time for signal to vanish) depends on the isothermal desorption temperature. The spectra in Fig. 7 were normalized for comparison (note the improving signal to noise ratio at higher temperature). The linear diffraction signal, recorded along with the QMS signal, decays roughly linearly during the xenon isothermal desorption period, with faster decay at higher temperature, reflecting the faster desorption rate as the temperature increases. The diffraction signal vanishes before the desorption process terminates, however linear diffraction traces exist down to monolayer thickness. The dependence of

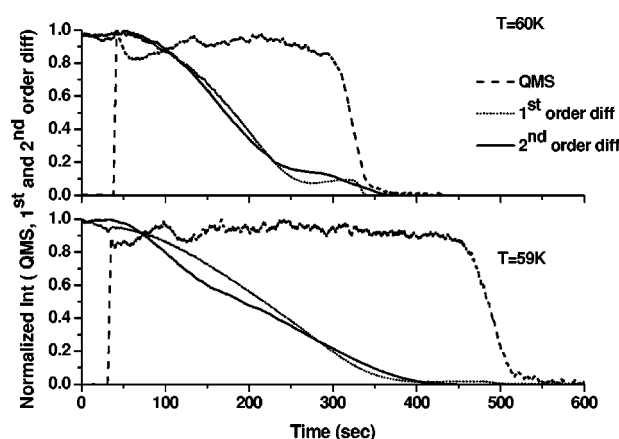


FIG. 8. Isothermal desorption vs the first- and second-order linear diffraction from a multilayer Xe coverage grating, at the indicated temperatures. Initial Xe coverage is 100 ML, heating rate from 20 K to the indicated temperature used for isothermal desorption was 3 K/s. The decay rate of the second-order diffraction is nearly identical to the first order, indicating that the shape of the grating pattern is effectively unchanged during the desorption process.

optical diffraction peak intensity on the Xe layer thickness is currently not well understood, but qualitatively its intensity increases linearly with the initial Xe layer thickness.

In order to confirm from yet another experimental point of view that no diffusion occurs on the surface prior to desorption of the multilayer xenon, the second-order linear diffraction signal was recorded both in isothermal and TPD modes, together with the mass spectrometer signal. If any diffusion takes place during the desorption process, the second-order signal should decay faster than the first order, as expected from Eq. (2), and has been demonstrated in the literature.^{33,36} Isothermal desorption spectra of 100 ML Xe from a coverage grating, recorded simultaneously with the second-order linear diffraction signal, are shown in Fig. 8. The decay signal of the first-order diffraction at identical parameters (i.e., same temperature, laser power for grating, and initial Xe coverage) is also shown, for comparison. Both signals decay at the same rate, and the intensity ratio of second/first diffraction peaks remains practically constant during the entire isothermal desorption of the multilayer Xe. This indicates that the profile of the grating pattern is conserved during the desorption process. In other words, no surface melting or diffusion takes place.

These experiments suggest the fact that the optical diffraction measurements from xenon coverage grating follow desorption rather than surface diffusion, as schematically presented in Fig. 4(b) versus Fig. 4(a). This can be considered a sublimative desorption process which may affect the growth mechanism of such noble gas layers on surfaces in general. Indeed, the lack of diffusion avoids any adsorbate 2D melting and rearrangement on the surface. For the reversed process of growth it may result in a rough three-dimensional (3D) growth (Stranski-Krastanov) rather than smooth layer by layer growth mode on solid surfaces. This means that the desorption mechanism and kinetics could depend on the growth mode. Indeed, using a retractable 1/4 in.

tube dozer of Xe instead of uniformly adsorbing Xe by back-filling the vacuum chamber with a leak valve, inhomogeneous deposition of the gas occurred. An erroneous fractional desorption order was obtained following this growth mode, as deduced from TPD and isothermal desorption measurements (not shown).

In spite of what is stated above, it needs to be emphasized that due to sensitivity limitations in our diffraction peak intensity measurements, we cannot rule out diffusion at the submonolayer level before the multilayer desorption has been completed.

D. Is sublimative desorption unique to Xe

A similar measurement has been performed using a 60 ML amorphous solid water (ASW) layer on top of the same Ru (100) sample. This is shown in Fig. 9. Very similar results were obtained, except that the temperature at which the diffraction signal starts to decay shifts toward the onset of ASW desorption near 150 K. The linear diffraction signal initiates its decay at the beginning of the water desorption process only. This suggests that the same sublimative desorption process dominates multilayer water desorption as well. Interestingly, the amorphous to crystalline phase transition of the ASW during heating and its initial desorption is clearly observed simultaneously by the mass spectrometer and very sensitively via the first-order linear diffraction signal. This is highlighted in the inset of Fig. 9.

These results indicate that sublimative desorption is not a process unique to multilayer Xe, but may be a general behavior of multilayer adsorbates on surfaces.

In both Xe and H₂O on the Ru surfaces, it is known that submonolayer adsorbates readily diffuse upon heating, namely a smaller barrier for diffusion than for desorption drives coverage gratings toward one-dimensional surface diffusion prior to desorption.^{27–38} In these cases one does not expect sublimative desorption as defined earlier.

The question arises how many layers are necessary in

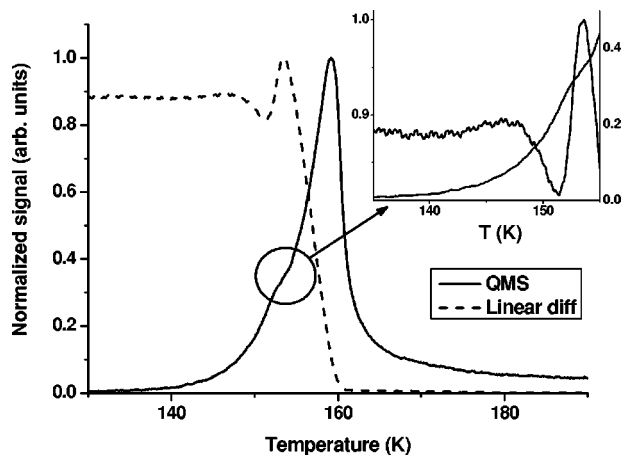


FIG. 9. Combined Δp -TPD with first-order optical linear diffraction signal from a coverage grating of 60 ML H₂O on Ru(100). Heating rate was 1 K/s.

order to shift the competing processes of diffusion (submonolayer) versus desorption (multilayers) in favor of sublimative desorption. We could not directly address this fundamental question due to experimental difficulties.

A simple estimate can, however, be made in order to evaluate this minimum number of layers. Consider a grating made of 50% covered area that is formed by four layers of Xe. If diffusion takes place, on average one may assume that the top two layers will cover the empty troughs of the grating. This will result in energy gain that is equivalent to the difference between the binding energy of the two first layers and that of the third layer (or more), all of them can be considered bound by the enthalpy of sublimation ($\Delta H_{\text{sub}} = 3.6$ kcal/mol). The first two layers are bound stronger, about the average value (ΔH_{av}) of the heat of adsorption of the first ($\Delta H_{\text{ads}} = 6.5$ kcal/mol) and the second layer ($\Delta H_{\text{ads}} \sim 4.8$ kcal/mol), resulting in $\Delta H_{\text{av}} = 5.6$ kcal/mol. If, however, the top two layers will desorb or sublime, the Gibbs free energy gain of the system will be entirely due to the entropy gain resulting from the change from solid to gas phase. This value can be estimated as $\Delta S_{\text{sub}}/\text{layer} = \Delta H_{\text{sub}}/T_{\text{sub}} = 3600/60 = 60$ cal/mol K layer. In order for the system to thermodynamically favor sublimation over diffusion, the free energy gain from sublimative desorption (given by the enthalpy of sublimation times the number of layers) should be larger than the enthalpy of adsorption (limited to the first two layers). It turns out that at least three layers are necessary for this condition to hold.

In a related experiment, concerned with collision-induced desorption of multilayers of ASW from Ru(001),^{39,40} it was concluded that at thicknesses above three to four layers, extraordinary stability and resilience against collision-induced desorption has been observed. It may therefore be that in the case of lateral motion and diffusion to smear out the coverage grating profile, at least three to four layers are necessary to make the thermodynamic switch that favors sublimative desorption over surface diffusion. It is expected that the number of layers necessary for favoring sublimative desorption would depend somewhat on the chemical nature of the adsorbate (strength of lateral attraction between neighbors) and also to a lesser extent on the coverage grating profile (that can be manipulated by the LITD laser power).

IV. CONCLUSIONS

The desorption of multilayer Xe from Ru(100) and its potential diffusion have been investigated, using TPD and isothermal desorption combined with optical linear diffraction from a multilayer Xe coverage modulation. Multilayer Xe desorption obeys zero-order rate law, as expected. However, the optical diffraction studies indicate that 2D melting and diffusion of the multilayer coverage modulation does not occur prior to or during desorption. It has been demonstrated that the decay of the optical linear diffraction signals follow a desorption process rather than diffusion. This behavior leads to the conclusion that Xe atoms sublimatively desorb from the multilayer structured Xe film without going through an intermediate surface “melting,” a typical step preceding submonolayer desorption from surfaces.

Similar behavior has been found with amorphous solid water multilayers on the same ruthenium surface. This observation suggests that the sublimative desorption defined here is in fact a rather general phenomenon characteristic of multilayer desorption kinetics from solid surfaces. The thermodynamic explanation for the lack of melting and diffusion in favor of sublimative desorption in multilayers is predicted to take over at layers thicker than 3 ML, in the cases of Xe and H₂O on Ru(100).

ACKNOWLEDGMENTS

We thank D. Menzel for stimulating discussions and his helpful comments. Fruitful discussion with A. Ben-Shaul is acknowledged. This work was partially supported by a grant from the US-Israel Binational Foundation and the Israel Science Foundation. The Farkas center for light induced processes is supported by the Bundesministerium für Forschung und Technologie and the Minerva Gesellschaft für die Forschung mbh.

*Corresponding author; Email address: asscher@fh.huji.ac.il

- ¹W. Widdra, P. Trischberger, W. Friess, D. Menzel, S. H. Payne, and H. J. Kreuzer, *Phys. Rev. B* **57**, 4111 (1998).
- ²H. Ulbricht, J. Kriebel, G. Moos, and T. Hertel, *Chem. Phys. Lett.* **363**, 252 (2002).
- ³H. Schlichting and D. Menzel, *Surf. Sci.* **272**, 27 (1992).
- ⁴H. Schlichting and D. Menzel, *Rev. Sci. Instrum.* **67**, 2013 (1993).
- ⁵C. T. Rettner, D. S. Bethune, and E. K. Schweizer, *J. Chem. Phys.* **92**, 1442 (1990).
- ⁶M. Bienfait and J. A. Venables, *Surf. Sci.* **64**, 425 (1977).
- ⁷J. C. Ruiz-Suarez, M. C. Vargas, F. O. Goodman, and G. Scoles, *Surf. Sci.* **243**, 219 (1991).
- ⁸H. J. Kreuzer and S. H. Payne, *Surf. Sci.* **200**, L433 (1988).
- ⁹J. A. Venables and M. Bienfait, *Surf. Sci.* **61**, 667 (1976).
- ¹⁰(a) B. Lehner, M. Hohage, and P. Zeppenfeld, *Chem. Phys. Lett.* **369**, 275 (2003); (b) *Surf. Sci.* **454–456**, 251 (2000).
- ¹¹K. L. Schmidt and K. Christmann, *Surf. Sci.* **492**, 167 (2001).
- ¹²R. G. Jones and D. L. Perry, *Surf. Sci.* **82**, 540 (1979).
- ¹³H. Asada and M. Masuda, *Surf. Sci.* **207**, 517 (1989).
- ¹⁴K. Nagay and A. Hirashima, *Surf. Sci.* **187**, L616 (1987).
- ¹⁵V. P. Zhdanov, *Surf. Sci.* **165**, L31 (1986).
- ¹⁶O. Sneh and S. M. George, *J. Chem. Phys.* **101**, 3287 (1994).
- ¹⁷P. Thomas, J. Gray, X. D. Zhu, and C. Y. Fong, *Chem. Phys. Lett.* **381**, 376 (2003).
- ¹⁸J. H. Weaver and G. D. Waddill, *Science* **251**, 1444 (1991).
- ¹⁹L. Huang, S. J. Chey, and J. H. Weaver, *Phys. Rev. Lett.* **80**, 4095 (1998).
- ²⁰V. N. Antonov and J. H. Weaver, *Surf. Sci.* **526**, 97 (2003).
- ²¹V. N. Antonov, J. S. Palmer, A. S. Bhatti, and J. H. Weaver, *Phys. Rev. B* **68**, 205418 (2003).
- ²²V. N. Antonov, J. S. Palmer, P. S. Waggoner, A. S. Bhatti, and J. H. Weaver, *Phys. Rev. B* **70**, 045406 (2004).
- ²³G. Kerner and M. Asscher, *Surf. Sci.* **557**, 5 (2004).
- ²⁴G. Kerner and M. Asscher, *Nano Lett.* **4**, 1433 (2004).
- ²⁵G. Kerner, Y. Horovitz, and M. Asscher, *J. Phys. Chem. B* **109**, 4545 (2005).
- ²⁶J. H. Weaver and V. N. Antonov, *Surf. Sci.* **557**, 1 (2004).
- ²⁷X. D. Zhu, A. Lee, A. Wong, and U. Linke, *Phys. Rev. Lett.* **68**, 1862 (1992).
- ²⁸X. D. Zhu and Y. R. Shen, *Opt. Lett.* **14**, 503 (1989).
- ²⁹X. D. Zhu, Th. Rasing, and Y. R. Shen, *Phys. Rev. Lett.* **61**, 2883 (1988).
- ³⁰P. W. Williams, G. A. Reider, L. P. Li, U. Höfer, T. Suzuki, and T. F. Heinz, *Phys. Rev. Lett.* **79**, 3459 (1997).
- ³¹W. Zhao, G. Kerner, M. Asscher, X. M. Wilde, K. Al-Shamery, H.-J. Freund, V. Staemmler, and M. Wieszbowska, *Phys. Rev. B* **62**, 7527 (2000).
- ³²V. S. Smentkowski and J. T. Yates, Jr., *J. Vac. Sci. Technol. A* **14**, 260 (1996).
- ³³R. W. Verhoef and M. Asscher, *Surf. Sci.* **376**, 389 (1997).
- ³⁴R. W. Verhoef and M. Asscher, *Surf. Sci.* **376**, 395 (1997).
- ³⁵(a) W. Zhao and M. Asscher, *J. Chem. Phys.* **107**, 5554 (1997); (b) *Surf. Sci.* **429**, 1 (1999).
- ³⁶Z. Rosenzweig, I. Farbman, and M. Asscher, *J. Chem. Phys.* **98**, 8277 (1993).
- ³⁷E. G. Seebauer and C. E. Allen, *Prog. Surf. Sci.* **49**, 265 (1995).
- ³⁸J. Ma, X. Xiao, N. J. DiNardo, and M. M. T. Loy, *Phys. Rev. B* **58**, 4977 (1998).
- ³⁹Y. Lilach, L. Romm, T. Livneh, and M. Asscher, *J. Phys. Chem. B* **105**, 2736 (2001).
- ⁴⁰M. Asscher and Y. Zeiri, *J. Phys. Chem. B* **107**, 6903 (2003).